

# New method for cotton fractional vegetation cover extraction based on UAV RGB images

Huanbo Yang<sup>1,2</sup>, Yubin Lan<sup>1,2</sup>, Liqun Lu<sup>2,3</sup>, Daocai Gong<sup>1,2</sup>, Jianchi Miao<sup>1,2</sup>, Jing Zhao<sup>1,2\*</sup>

(1. School of Agricultural and Food Engineering, Shandong University of Technology, Zibo 255000, Shandong, China;

2. International Precision Agriculture Aviation Application Technology Research Center, Shandong University of Technology, Zibo 255000, Shandong, China;

3. School of Transportation and Vehicle Engineering, Shandong University of Technology, Zibo 255000, Shandong, China)

**Abstract:** As the key principle of precision farming, the distribution of fractional vegetation cover is the basis of crop management within the field serves. To estimate crop FVC rapidly at the farm scale, high temporal-spatial resolution imagery obtained by unmanned aerial vehicle (UAV) was adopted. To verify the application potential of consumer-grade UAV RGB imagery in estimated FVC, blue-green characteristic vegetation index (TBVI) and red-green vegetation index (TRVI) were proposed in this study according to the differences of the gray value among cotton vegetation, soil and shadow in the field. First, two new constructed indices and several published indices were used to extract visible light images and generate greyscale images for each of the visible light vegetation indices. Then, the thresholds of cotton vegetation and non-vegetation pixels were established based on the vegetation index threshold method which combines support vector machine classification and vegetation index. Finally, the accuracy difference in vegetation information extraction between the newly constructed and several published indices was compared. The results show that the accuracy of the information extracted by TRVI is higher than that of subdivision index of other visible light (FVC extraction precision in the first bud stage of cotton:  $R^2=0.832$ ,  $RMSE=2.307$ ,  $nRMSE=4.405\%$ ; FVC extraction precision in the bud stage of cotton:  $R^2=0.981$ ,  $RMSE=1.393$ ,  $nRMSE=1.984\%$ ; FVC extraction precision in the flowering stage of cotton:  $R^2=0.893$ ,  $RMSE=2.101$ ,  $nRMSE=2.422\%$ ; FVC extraction precision in the boll stage of cotton:  $R^2=0.958$ ,  $RMSE=1.850$ ,  $nRMSE=2.050\%$ ).

**Keywords:** cotton, UAV, visible light images, fractional vegetation cover, vegetation index threshold method, TRVI, TBVI

**DOI:** 10.25165/j.ijabe.20221504.6207

**Citation:** Yang H B, Lan Y B, Lu L Q, Gong D C, Miao J C, Zhao J. New method for cotton fractional vegetation cover extraction based on UAV RGB images. *Int J Agric & Biol Eng*, 2022; 15(4): 172–180.

## 1 Introduction

Cotton is China's main cash crop<sup>[1,2]</sup>, involves commodities in two major industries of textile and agriculture, which is the main source of income for 100 million cotton farmers. In recent years, the cotton planting area in China has declined significantly, especially in the Yellow River Basin. Complex cotton planting and management procedures, high costs, and long growth cycles are the main reasons for the decline of cotton planting area. Accurate and effective management of cotton in the field, adjustment of the amount of fertilization and irrigation, rational planning of cotton layout, and optimization of cotton planting and breeding techniques are crucial to the development of the cotton industry.

Fraction vegetation cover (FVC) is defined as the vertical projection of the crown or shoot area of vegetation canopies from the ground surface, and is expressed as a fraction or percent of the reference area<sup>[3,4]</sup>, which is closely related to crop growth and yield information<sup>[5,6]</sup>. Reasonable monitoring of cotton FVC is of great significance to the crop management. At present, high-resolution (HR) remote sensing images have been widely used in many fields to obtain spatial information<sup>[7-9]</sup>, which provide more accurate information source for vegetation information monitoring. The use of remote sensing images is more convenient for extracting and monitoring vegetation information in the field scale<sup>[10-12]</sup>. Common FVC extraction mainly includes vegetation index threshold method, linear spectral mixed mode, machine learning and regression model<sup>[13]</sup>. The common features of these FVC extraction methods are that the higher image resolution, the higher accuracy of crop FVC extraction. However, satellite remote sensing data is not applicable for the accurate extraction of FVC of field-scale crops because of the low resolution and time lag defects of satellite remote sensing images<sup>[14]</sup>. In addition, restricted by material conditions, the remote sensing data obtained by ground remote sensing is difficult to apply to the extraction of crop FVC in large areas.

With the rapid development of technology<sup>[15]</sup>, UAV remote sensing is widely used in the extraction of FVC<sup>[16-19]</sup>. UAV remote sensing has the advantages of low cost, simple operation, and high ground resolution<sup>[20]</sup>, which is incomparable with traditional remote sensing technologies<sup>[21,22]</sup>. UAV has become an indispensable means for remote sensing monitoring of vegetation

**Received date:** 2020-10-09 **Accepted date:** 2022-05-14

**Biographies:** **Huanbo Yang**, PhD, research interests: agricultural remote sensing and intelligent detection, Email: 1332616134@qq.com; **Yubin Lan**, PhD, research interests: precision agriculture aviation, Email: ylan@sdut.edu.cn; **Liqun Lu**, PhD, Associate Professor, research interests: agricultural aviation and fluid transmission, Email: luliqunustb@163.com; **Daocai Gong**, Master candidate, research interests: agricultural remote sensing and intelligent detection, Email: 1252128352@qq.com; **Jianchi Miao**, Master candidate, research interests: agricultural remote sensing and intelligent detection, Email: 1393746086@163.com.

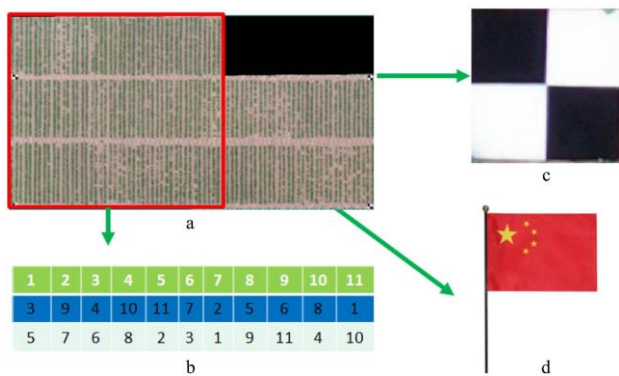
\***Corresponding author:** **Jing Zhao**, PhD, Associate Professor, research interests: agricultural remote sensing and intelligent detection. Shandong University of Technology, No. 266 Xincun West Road, Zhangdian District, Zibo 255000, Shandong, China. Tel: +86-13792194725, Email: zbceozj@163.com.

information<sup>[23]</sup>. So far, most vegetation indices are constructed based on the low reflectance of green plants in the visible band and the high reflectance in the near-infrared band<sup>[24]</sup>. Presently, most mainstream UAVs on the market are equipped with visible light digital cameras, and thus, the vegetation indices composed of the traditional visible light and near-infrared band cannot be applied. A variety of visible light vegetation indices utilizing the spectral reflectance characteristics of green vegetation in the visible light band have been constructed. However, most of the vegetation indexes above in the visible band do not consider the spectral difference between vegetation and soil, and the shadow spectrum. So, the real-time extraction and analysis of field vegetation information using UAV visible light remote sensing images cause big errors. In order to eliminate the influence of shadow on the FVC extraction of crops, the spectral characteristics of visible light band for soil, vegetation and shadow will be analyzed, and the TBVI and TRVI will be creatively constructed in this study.

## 2 Materials and methods

### 2.1 Research field

The experiments are carried out on a field in Linqing city located in the northwest of Shandong Province, China. Linqing city is a national temperate monsoon climate area of warm temperate zone. Eleven types of cotton in the test were high-yield, lodging-resistant fine varieties independently cultivated by Shandong Cotton Testing Center. Cotton was planted by machine in April 2019, and the visible light images of cotton were collected in the first bud stage, bud stage, flowering stage and boll stage. Four reference plates were arranged in the test area for geometric correction. The research field was approximately 1333 m<sup>2</sup>. An overview of the research field is shown in Figure 1.



Note: Figure 1a shows a panoramic view of the experimental field; Figure 1b shows the reference plate for ground geometric correction; Figure 1c demonstrates the cotton variety distribution map, and Figure 1d displays the red flag in the sampling area.

Figure 1 Schematic diagram of experimental field distribution

### 2.2 Collecting and splicing of UAV remote sensing images

The experiment data were collected by the UAV visible light remote sensing images at a resolution of 0.8 cm. During this experiment, Mavic 2 Pro (Shenzhen Dajiang Baiwang Technology Co., Ltd., Shenzhen, China) was adopted to collect visible light images of cotton in the first bud stage, bud stage, flowering stage and boll stage, which had a remote sensing platform with a CMOS digital camera to perform over 30 min. The camera had a 77° field of view lens with an f/2.8-f/11 aperture and a resolution of 5472×3648 pixels. The digital camera was de-noised, and lens distortion correction was performed before using. Its main parameters are shown in Table 1. In order to reduce the impact of light changes on the visible light images of cotton obtained by the

UAV, the visible light images of the four periods of cotton were performed at around 12:00 pm. in sunny and windless weather. Flight was controlled by Altizure software (Everest Innovation Technology Ltd., Hong Kong, China), which directed the UAV flying along with a serpentine image acquisition plan at a height of 30 m and a speed of 3 m/s with the downward-looking pose. Overlap of image to the front and side was 90%, and 365 visible light images of cotton were collected in each period. To improve the geo-location accuracy, the geo-referencing of the point clouds was done using a combination of direct geo-referencing and 4 ground control points.

Table 1 Performance parameters of UAV

|               |  |
|---------------|--|
| Aperture      | f/2.8-f/11                               |
| Speed         | 72 km/h                                  |
| ISO range     | 100-3200 (automatic), 100-12800 (Manual) |
| Shutter speed | 8-1/8000s                                |
| Camera model  | L1D-20c                                  |
| Flight time   | 31min                                    |

After collecting images, the image mosaic processing was performed by using Agisoft PhotoScan Professional software. It is a UAV aerial photography processing software developed by Russia, which could process images in multiple formats according to the latest multi-view 3D reconstruction technology. The processing started with aligning the cotton visible light image obtained by the UAV based on the coordinate information of route. After that, mesh was generated, and 4 ground control points were incorporated to correct the geographic coordinates of images. Then meshes and textures of visible light images of cotton were generated. Finally, the digital surface model and orthophoto were obtained by the inverse distance weighting method.

### 2.3 Selection of the UAV remote sensing visible vegetation index

Compared with the hyperspectral and multispectral remote sensing systems carried by UAV, the UAV visible light remote sensing system contains less band information, but it has advantages of easy collection, low cost and high spatial resolution, which is convenient for ordinary farmers. The common visible light band vegetation indices were constructed based on the strong reflection of vegetation in the green band and the absorption in the yellow and blue bands. In this study, VIs were calculated using visible bands, including the GLI<sup>[25]</sup>, NGBDI<sup>[26]</sup>, GRVI<sup>[27]</sup> and EXG<sup>[28]</sup>. The calculation formulas are shown as follows.

$$GLI = \frac{2G - R - B}{2G + R + B} \tag{1}$$

$$NGBDI = \frac{G - B}{G + B} \tag{2}$$

$$GRVI = \frac{G - R}{G + R} \tag{3}$$

$$EXG = 2G - R - B \tag{4}$$

where, *G*, *R*, and *B* represent the digital numbers of red, green, and blue bands which are normalized by dividing 255.

### 2.4 Construction of the TBVI and TRVI

Considering the cotton growing vigorously in the bud stage, flowering stage and boll stage, the shadow area was large. In order to reduce the influence of the shadow on the FVC extraction of the bud stage, flowering stage and boll stage, 80 regions of interest (ROI) for cotton, soil and shadow were selected on the orthographic image of cotton bud stage. The eigenvalues (including maximum, minimum, average and standard deviation) of the pixels in the red, green and blue bands of cotton, soil and

shadow samples were counted. The mean was selected as an index for evaluating the overall difference of the three bands of cotton, soil and shadow, and the standard deviation was introduced to view the fluctuation range of each band. The results are listed in Table 2.

**Table 2 Table of cotton vegetation, soil and shadow pixel value difference in blue, green and red bands**

| Typical objects | Blue band |                    | Green band |                    | Red band |                    |
|-----------------|-----------|--------------------|------------|--------------------|----------|--------------------|
|                 | mean      | standard deviation | mean       | standard deviation | mean     | standard deviation |
| cotton          | 95.8907   | 35.1928            | 134.1354   | 36.1976            | 64.0713  | 31.7151            |
| soil            | 197.7362  | 19.2597            | 167.8074   | 19.9035            | 127.3901 | 22.2801            |
| shadow          | 58.1999   | 12.9624            | 57.0575    | 11.1267            | 44.0674  | 10.9475            |

Table 2 shows that the gray values of cotton and soil in the blue and red bands crossed, and the gray values of cotton vegetation and the soil in the green band crossed. It was difficult to identify cotton vegetation from the soil and shadow through a single band. Therefore, the red, green and blue band differences corresponding to cotton, soil and shadow features are found through band combination, then new features are constructed to extract cotton FVC, and the scatter map of cotton, soil and shadow

red, green and blue gray value combination is constructed. The scatter plots of the combination of red, green and blue greyscale values for cotton, soil and shadow were built. The scatter plots of the combination of red-green and green-blue greyscale values for cotton, soil and shadow were selected based on the apparent dividing line between cotton, soil and shadow (Figure 2). As shown in Figure 2, there are two clear boundaries between cotton, soil and shadow scatter plots based on red-green and blue-green axes. Cotton is basically distributed at the upper left of the boundary lines, while the soil and shadow are basically distributed at the lower right of the boundary. The dividing line scatter coordinate value was extracted by the visual interpretation method. Sixty points are read on the two scatter plots for fitting, and then the expression of feature combination parameters can be obtained. The fitting results are shown in Figure 3. The fitted boundary function expressions are taken as the newly constructed vegetation index TBVI and TRVI, and the TBVI and TRVI formulas are shown in Equations (5) and (6). The greyscale images of TBVI and TRVI are shown in Figure 4. The correlation coefficient of the 6 vegetation indices are shown in Figure 5.

$$TBVI = G - 1.2531B - 34.446 \tag{5}$$

$$TRVI = G - 1.0635R - 15.81 \tag{6}$$

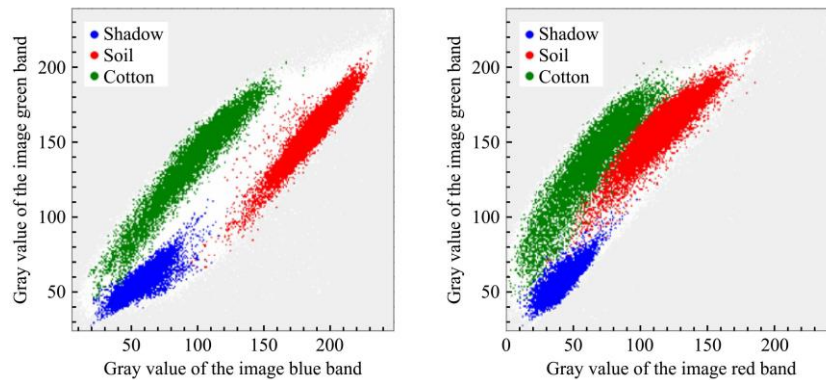


Figure 2 Characteristics of cotton, soil and shadow distribution under different wave band combinations

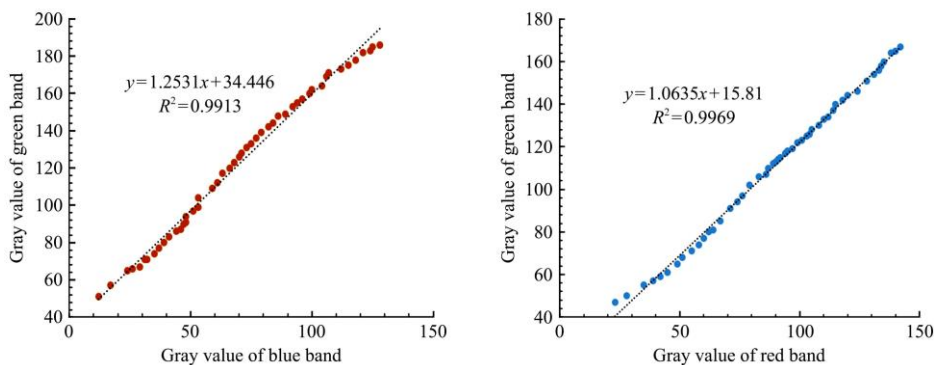


Figure 3 Fitting results of cotton vegetation boundary

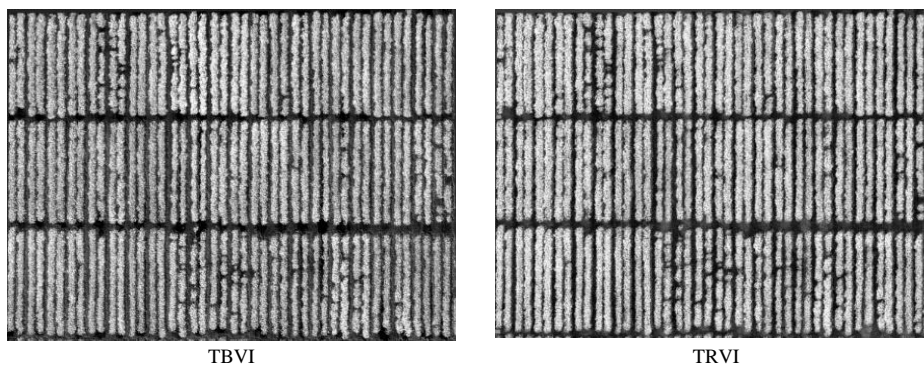


Figure 4 Greyscale images of TBVI and TRDI



Figure 5 Correlation coefficient of the 6 vegetation indices

### 2.5 Extraction technology of vegetation information based on vegetation index threshold method

#### 2.5.1 Vegetation index threshold method

The vegetation index threshold method was constructed in this study to extract the FVC information of cotton combining the time series intersection threshold method and sample statistics method. Vegetation index time series intersection method<sup>[28]</sup> believed that the research field was composed of vegetation and soil. With the continuous growth of crops, the number of vegetation pixels in the experimental field continued to increase, and the increasing number of vegetation pixels came from the decreasing number of soil pixels. Therefore, the intersection of the vegetation index for the area with high FVC and the area with low FVC could be used as the threshold for the extraction of crop FVC. The sample statistical method<sup>[29]</sup> performed statistical analysis on the basis of visual interpretation, and then determined the extraction threshold of crop FVC. The orthophotos of cotton in a certain period were divided into soil and vegetation by supervised classification. Histogram of cotton vegetation and soil vegetation index in supervised classification was counted, and the intersection of soil and cotton vegetation index was used as the threshold of cotton FVC extraction.

With the growth of cotton, there were a lot of shadows in the visible light remote sensing images of the research field after the cotton first bud stage, and the environment of the research field became more complicated. If the FVC threshold determined by the vegetation index threshold method in the first bud stage of cotton used to extract the cotton FVC in bud stage, flowering stage and boll stage, there would be a large error in the extraction of cotton vegetation. Therefore, the threshold value of the cotton first bud stage determined by the vegetation index threshold method was only used to extract the FVC of the cotton first bud stage. The threshold value of the cotton buds stage determined by the vegetation index threshold method was used to extract cotton FVC in the bud stage, flowering stage, and boll stage.

In order to improve the efficiency of the vegetation index threshold method for extracting the FVC of cotton, some areas were cropped on the orthophotos of the experimental field in the first bud stage and the bud stage of the cotton using support vector machine classification.

#### 2.5.2 Verification method of cotton FVC extraction accuracy

With the development of machine learning and remote sensing technology, the use of supervised classification results as the true value of FVC for extraction accuracy evaluation has been widely used. Therefore, the cotton FVC extracted by the support vector

machine was selected as the true value to verify the accuracy of the cotton FVC extracted by the vegetation index threshold method. The verification process was divided into two parts. First, the overall extraction accuracy of cotton FVC in the research field was verified by the error calculation of Equation (7), and the vegetation indices with large error were eliminated. The model indicators of decision coefficient ( $R^2$ ), root mean square error ( $RMSE$ ) and normalized root mean square error ( $nRMSE$ ) were applied to evaluate the FVC extraction results of vegetation index with less residual error. Finally, suitable vegetation indices were selected to extract FVC of cotton in the first bud stage, the bud stage, the flowering stage and the boll stage of cotton.

$$E_F = \frac{|F_{sup} - F_{VI}|}{F_{sup}} \times 100\% \tag{7}$$

where,  $E_F$  is the error of FVC extraction;  $F_{sup}$  is cotton FVC results extracted by Random Forest or SVM;  $F_{VI}$  is cotton FVC results extracted by vegetation index threshold method.

## 3 Results

### 3.1 Extraction threshold of cotton FVC based on vegetation index threshold method

The orthophotos of the cotton in the first bud stage and bud stage were cropped. 80 regions of interests for cotton and soil were selected from the cropped orthophoto as training sets for Random Forest classification, and 60 regions of interests for cotton and soil were selected as verification sets to verify the Random Forest classification results. The separability between cotton and soil samples of orthophotos in the first bud stage in the training set was 1.997, and the separability between cotton and soil samples of orthophotos in the bud stage in the training set was 1.998. Supervised classification results are shown in Figure 6.

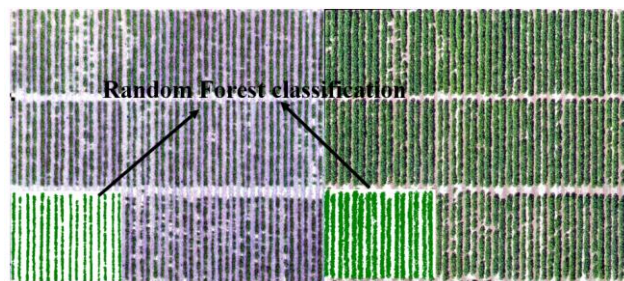


Figure 6 Random Forest classification results of cotton in the first bud stage and bud stage

The confusion matrix was used to verify the classification accuracy of Random Forest. The overall classification accuracy of cotton in the first bud stage was 99.4339%, and the Kappa coefficient was 0.9887. The overall classification accuracy of cotton in the bud stage was 99.9625%, and the Kappa coefficient was 0.9991. The verification results of the confusion matrix in the first bud stage and bud stage of cotton are listed in Tables 3 and 4. From the verification results of the confusion matrix, it could be seen that the Random Forest classification achieved high accuracy.

**Table 3 Verification results of confusion matrix for cotton Random Forest classification in first bud stage**

| Typical objects               | Soil/pixel | Cotton/pixel | Total number of samples/pixel | User precision/% |
|-------------------------------|------------|--------------|-------------------------------|------------------|
| Soil                          | 25278      | 275          | 25553                         | 98.92            |
| Cotton                        | 11         | 24957        | 24968                         | 99.96            |
| Total number of samples/pixel | 25289      | 25232        | 50521                         |                  |
| Prod precision/%              | 99.96      | 98.91        |                               |                  |

**Table 4 Verification results of confusion matrix for cotton Random Forest classification in bud stage**

| Typical objects               | Soil/pixel | Cotton/pixel | Total number of samples/pixel | User precision/% |
|-------------------------------|------------|--------------|-------------------------------|------------------|
| Soil                          | 49157      | 6            | 49163                         | 99.99            |
| Cotton                        | 20         | 20215        | 20235                         | 99.90            |
| Total number of samples/pixel | 49177      | 20221        | 69398                         |                  |
| Prod precision/%              | 99.96      | 99.97        |                               |                  |

The six vegetation indices of cotton vegetation and soil in the classification results were counted in the first bud and the bud stage of cotton. Statistical histogram of soil and cotton are shown by using the vegetation index values of soil and cotton as the abscissa

and the number of pixel statistics as the ordinate. The intersection point of cotton and soil for the 6 vegetation indices under the coordinate system was used as the classification threshold of cotton and soil. Figures 7 and 8 show the statistics histogram of the 6 vegetation indices above in the first bud stage and in the bud stage of cotton, respectively.

The FVC extraction thresholds of TRVI, EXG, GLI, NGBDI, GRVI and TBVI in the first bud stage of cotton extracted by the vegetation index threshold method were -16.8468, 26.7898, 0.0570, 0.0846, 0.0255 and -41.3817, respectively. The extracting thresholds of FVC in the bud stage, flowering stage and boll stage of cotton were -11.0260, 48.2900, 0.1183, 0.2176, 0.0289 and -10.2554, respectively.

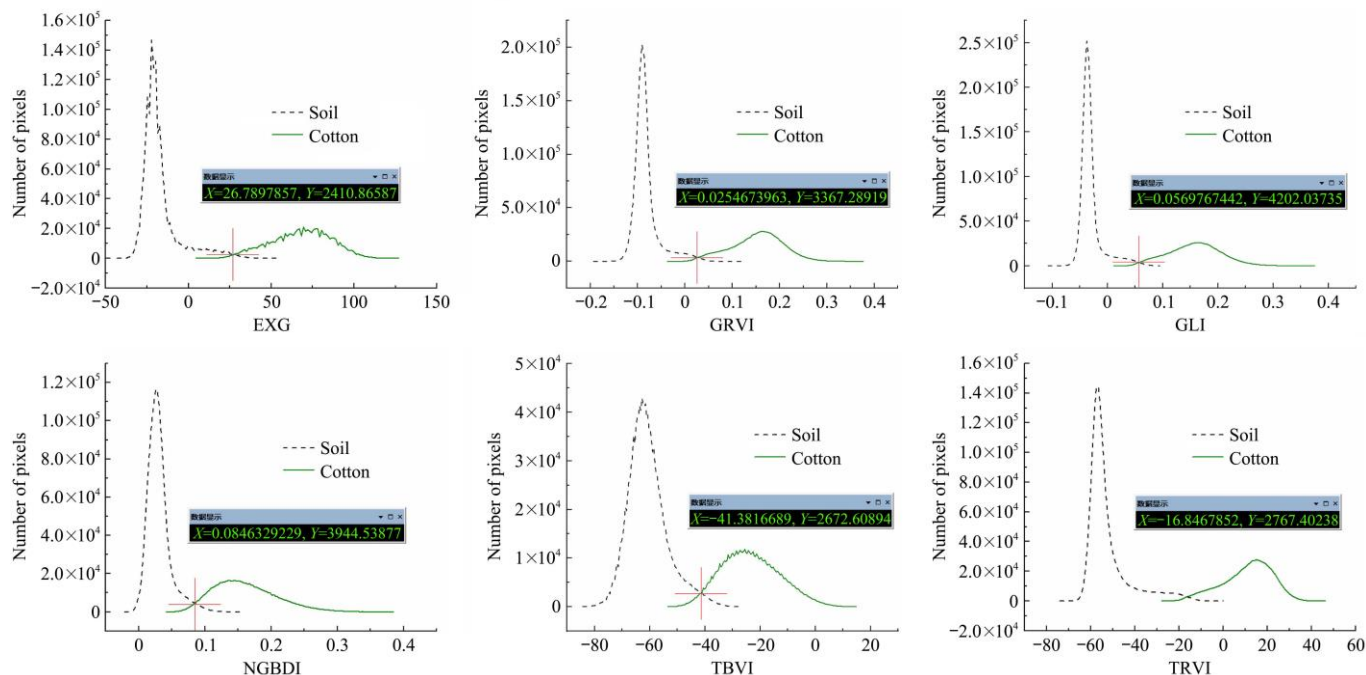


Figure 7 Threshold extraction results of vegetation indices in first bud stage of cotton

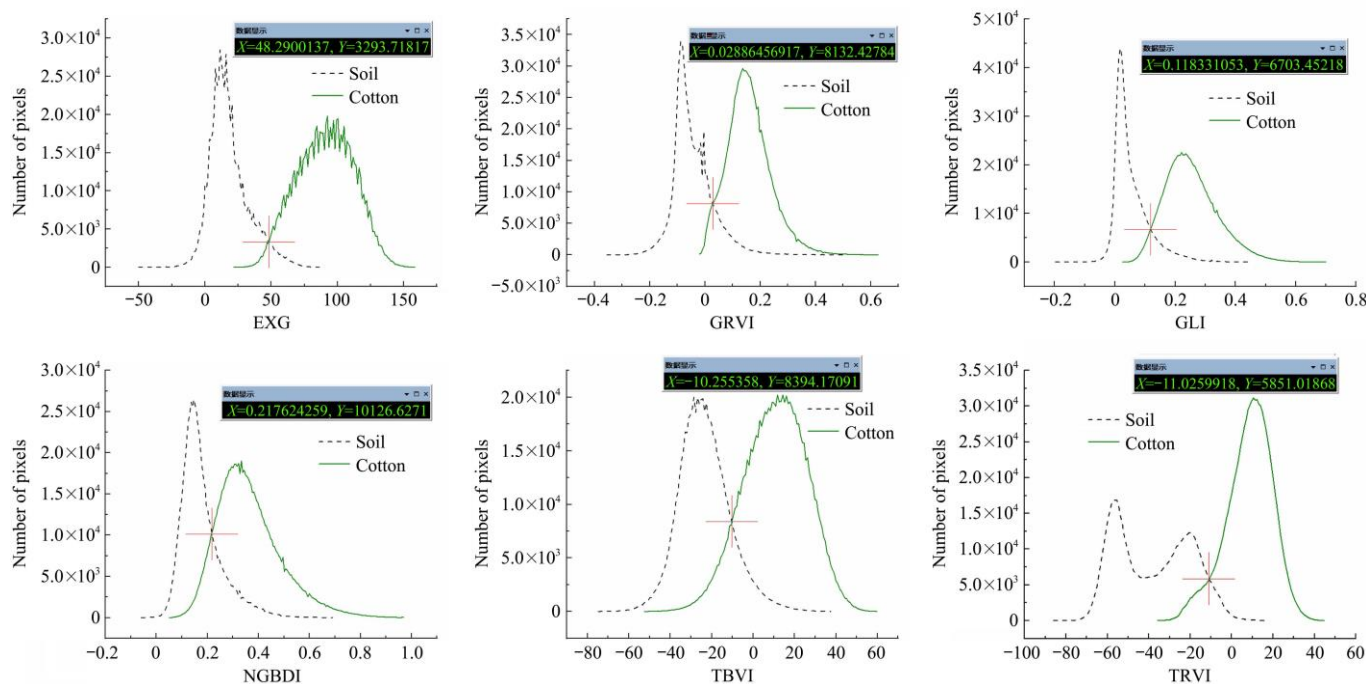


Figure 8 Threshold extraction results of vegetation indices in bud stage of cotton

**3.2 Extraction results of cotton FVC**

The FVC extraction threshold of the cotton corresponding

stage determined in the cropped image above was used to extract FVC of entire research field. The FVC extraction results of the

first bud stage, the bud stage, the flowering stage and the boll stage were obtained by Equation (8). The results of FVC extraction are listed in Table 5.

$$FVC = \frac{N_{cotton}}{N_{cotton} + N_{soil}} \quad (8)$$

where,  $N_{cotton}$  is count of cotton pixels;  $N_{soil}$  is count of soil pixels.

**Table 5 Extraction results of cotton FVC based on vegetation index threshold method**

| Growth stage of cotton | Vegetation index | Extraction results of FVC/% | Vegetation index | Extraction results of FVC/% |
|------------------------|------------------|-----------------------------|------------------|-----------------------------|
| First bud stage        | GLI              | 29.9836                     | GRVI             | 30.3058                     |
| Buds stage             |                  | 57.7577                     |                  | 58.1896                     |
| Flowering stage        |                  | 82.2432                     |                  | 81.7456                     |
| Boll stage             |                  | 93.8881                     |                  | 93.6949                     |
| First bud stage        | NGBDI            | 29.8299                     | TBVI             | 29.3734                     |
| buds stage             |                  | 59.3726                     |                  | 55.5979                     |
| Flowering stage        |                  | 77.9169                     |                  | 68.8122                     |
| Boll stage             |                  | 88.8677                     |                  | 89.8567                     |
| First bud stage        | EXG              | 30.2755                     | TRVI             | 30.2321                     |
| buds stage             |                  | 55.9740                     |                  | 53.2683                     |
| Flowering stage        |                  | 72.9375                     |                  | 78.2825                     |
| Boll stage             |                  | 91.3325                     |                  | 92.1693                     |

**3.3 Verification of Extraction Precision of Cotton FVC**

Random forest and SVM which have higher accuracy in cotton coverage extraction were used to verify the accuracy of vegetation index threshold method. The Random Forest and SVM classification verification results of the 4 grow stages of cotton are shown in Tables 6 and 7.

**Table 6 Verification results of the confusion matrix accuracy of Random Forest classification in four periods of cotton**

| Growth stage of cotton | The accuracy of cotton classification results | The accuracy of soil classification results | Total accuracy of classification results | Kappa coefficient |
|------------------------|---|---|--|-------------------|
| First bud stage        | 99.51   | 99.82                                       | 99.79                                    | 0.996             |
| Buds stage             | 99.34   | 99.96                                       | 99.72                                    | 0.995             |
| Flowering stage        | 98.14   | 90.54                                       | 99.31                                    | 0.886             |
| Boll stage             | 99.98   | 99.91                                       | 99.94                                    | 0.998             |

**Table 7 Verification results of the confusion matrix accuracy of SVM classification in four periods of cotton**

| Growth stage of cotton | The accuracy of cotton classification results | The accuracy of soil classification results | Total accuracy of classification results | Kappa coefficient |
|------------------------|---|---|--|-------------------|
| First bud stage        | 99.38   | 99.75                                       | 99.64                                    | 0.993             |
| Buds stage             | 99.17   | 99.97                                       | 99.69                                    | 0.996             |
| Flowering stage        | 99.95   | 99.34                                       | 99.73                                    | 0.994             |
| Boll stage             | 99.94   | 99.77                                       | 99.84                                    | 0.996             |

Through the comparison of the above two methods, it can be seen that the FVC accuracy of random forest algorithm in cotton initial bud stage, full bud stage and boll stage is higher, and that of SVM in cotton flowering stage is higher. Therefore, the FVC results of cotton in first bud stage, bud stage and boll stage extracted by Random Forest, and the FVC results of cotton in flowering stage extracted by SVM are used as true values to verify the cotton coverage extracted by vegetation index threshold method.

The verification results of the overall cotton FVC extracted by the vegetation index threshold method are listed in Table 8.

**Table 8 Overall verification results of cotton FVC extraction accuracy based on vegetation index threshold method**

| Vegetation index | Growth stage of cotton | Vegetation index threshold method (FVC) | Supervised classification results | Extraction error/% | Absolute error |
|------------------|------------------------|---|-----------------------------------|--------------------|----------------|
| GLI              | 1                      | 0.2998                                  | 0.3143                            | 4.6134             | 0.0145         |
|                  | 2                      | 0.5776                                  | 0.5377                            | 7.4205             | 0.0399         |
|                  | 3                      | 0.8224                                  | 0.7655                            | 7.4331             | 0.0569         |
|                  | 4                      | 0.9389                                  | 0.9040                            | 3.8606             | 0.0349         |
| EXG              | 1                      | 0.3028                                  | 0.3143                            | 3.6589             | 0.0115         |
|                  | 2                      | 0.5597                                  | 0.5377                            | 4.0915             | 0.022          |
|                  | 3                      | 0.7294                                  | 0.7655                            | 4.7159             | 0.0361         |
|                  | 4                      | 0.9133                                  | 0.9040                            | 1.0288             | 0.0093         |
| NGBDI            | 1                      | 0.2983                                  | 0.3143                            | 5.0907             | 0.016          |
|                  | 2                      | 0.5937                                  | 0.5377                            | 10.4147            | 0.056          |
|                  | 3                      | 0.7792                                  | 0.7655                            | 1.7897             | 0.0137         |
|                  | 4                      | 0.8887                                  | 0.9040                            | 1.6925             | 0.0153         |
| GRVI             | 1                      | 0.3031                                  | 0.3143                            | 3.5635             | 0.0112         |
|                  | 2                      | 0.5819                                  | 0.5377                            | 8.2202             | 0.0442         |
|                  | 3                      | 0.8175                                  | 0.7655                            | 6.7929             | 0.052          |
|                  | 4                      | 0.9369                                  | 0.9040                            | 3.6394             | 0.0329         |
| TRVI             | 1                      | 0.3023                                  | 0.3143                            | 3.8180             | 0.012          |
|                  | 2                      | 0.5327                                  | 0.5377                            | 0.9299             | 0.005          |
|                  | 3                      | 0.7828                                  | 0.7655                            | 2.2600             | 0.0173         |
|                  | 4                      | 0.9217                                  | 0.9040                            | 1.9580             | 0.0177         |
| TBVI             | 1                      | 0.2937                                  | 0.3143                            | 6.5542             | 0.0206         |
|                  | 2                      | 0.5560                                  | 0.5377                            | 3.4034             | 0.0183         |
|                  | 3                      | 0.6881                                  | 0.7655                            | 10.1110            | 0.0774         |
|                  | 4                      | 0.8986                                  | 0.9040                            | 0.5973             | 0.0054         |

Note: Stage 1 means the first bud stage of cotton, Stage 2 means the bud stage of cotton, Stage 3 means the flowering stage of cotton, Stage 4 means the boll stage of cotton.

Although the above-mentioned six vegetation indices had different results in the extraction of FVC in different growing stages of cotton, the extraction accuracy of FVC based on EXG, TRVI and TBVI were higher than those of other vegetation indices. 33 samples were selected to verify the local FVC results of EXG, TRVI and TBVI. The verification results of FVC extraction in the four stages of cotton are shown in Figures 9-12.

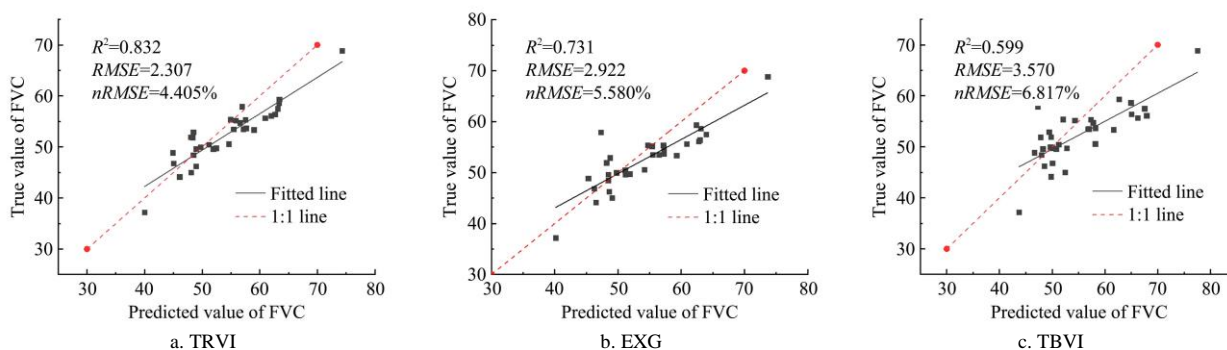


Figure 9 Verification results of cotton FVC extraction precision in first bud stage

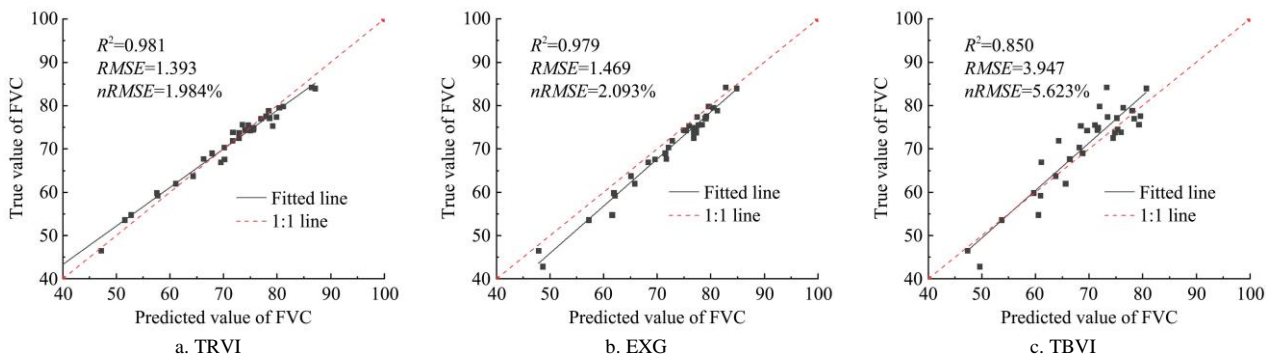


Figure 10 Verification results of cotton FVC extraction precision in bud stage

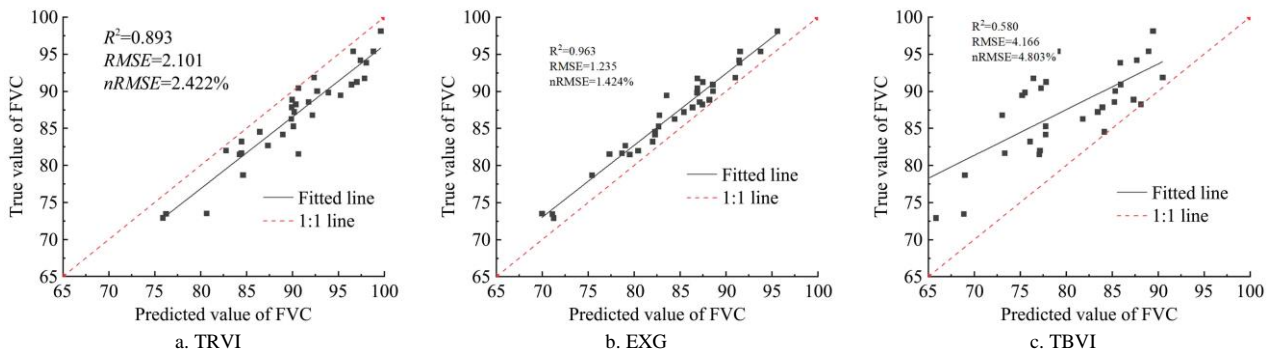


Figure 11 Verification results of cotton FVC extraction precision in flowering stage

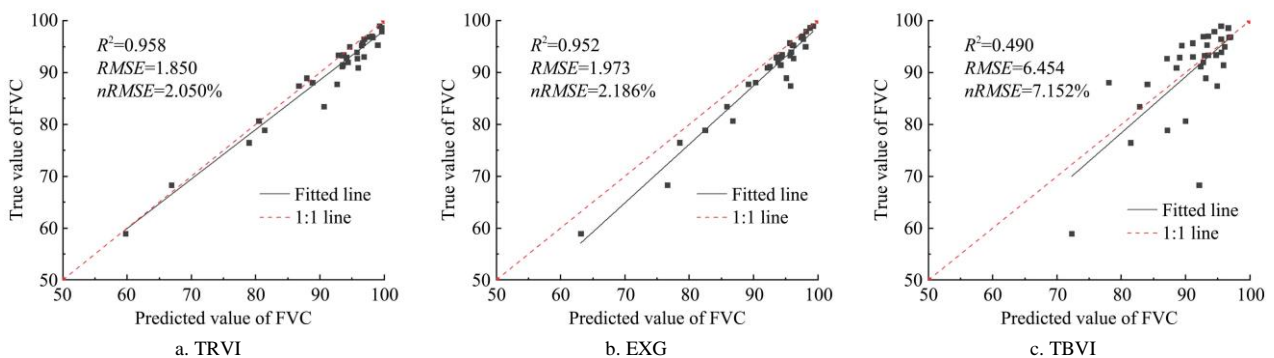


Figure 12 Verification results of cotton FVC extraction precision in boll stage

The accuracy of cotton FVC extracted by TRVI vegetation index threshold method was the highest ( $R^2=0.832$ ,  $RMSE=2.307$ ,  $nRMSE=4.405\%$ ), followed by EXG vegetation index threshold method ( $R^2=0.731$ ,  $RMSE=1.469$ ,  $nRMSE=5.580\%$ ) and TBVI vegetation index threshold method ( $R^2=0.599$ ,  $RMSE=3.570$ ,  $nRMSE=6.817\%$ ) in the first bud stage of cotton.

The accuracy of cotton FVC extracted by TRVI vegetation index threshold method was the highest ( $R^2=0.981$ ,  $RMSE=1.393$ ,  $nRMSE=1.984\%$ ), followed by EXG vegetation index threshold method ( $R^2=0.979$ ,  $RMSE=1.469$ ,  $nRMSE=2.093\%$ ). The accuracy of cotton FVC extracted by TBVI vegetation index threshold method was lowest ( $R^2=0.850$ ,  $RMSE=3.947$ ,  $nRMSE=5.623\%$ ) in the bud stage of cotton.

The accuracy of cotton FVC extracted by EXG vegetation index threshold method was the highest ( $R^2=0.963$ ,  $RMSE=1.235$ ,  $nRMSE=1.424\%$ ), followed by TRVI vegetation index threshold method ( $R^2=0.893$ ,  $RMSE=2.101$ ,  $nRMSE=2.422\%$ ). The accuracy of cotton FVC extracted by TBVI vegetation index threshold method was lowest ( $R^2=0.580$ ,  $RMSE=4.166$ ,  $nRMSE=4.803\%$ ) in the flowering stage of cotton.

The accuracy of cotton FVC extracted by TRVI vegetation index threshold method was the highest ( $R^2=0.958$ ,  $RMSE=1.850$ ,  $nRMSE=2.050\%$ ), followed by EXG vegetation index threshold

method ( $R^2=0.952$ ,  $RMSE=1.973$ ,  $nRMSE=2.186\%$ ). The accuracy of cotton FVC extracted by TBVI vegetation index threshold method was lowest ( $R^2=0.490$ ,  $RMSE=6.454$ ,  $nRMSE=7.152\%$ ) in the growth stage of cotton boll stage.

The FVC accuracy of the cotton first bud, buds and boll stages extracted by the TRVI vegetation index threshold method was highest. The accuracy of the cotton FVC in the flowering stage extracted by the TRVI vegetation index threshold method was slightly lower than that by the EXG vegetation index threshold method. In view of the verification results of FVC extraction accuracy, TRVI vegetation index threshold method was selected to extract the FVC of cotton in the above-mentioned four periods. The results of FVC extraction are shown in Figure 13.

## 4 Discussion

When it comes to monitoring FVC by using VIs, there are two traditionally data sources, satellite remote sensing<sup>[30-32]</sup> and Near-Earth remote sensing<sup>[33-35]</sup>. Because satellite remote sensing is limited by image resolution and effectiveness, and ground remote sensing technology is limited by human and material conditions, the two remote sensing methods are difficult to apply to field-level FVC monitoring. The UAV visible light remote sensing system has been widely used in the field of FVC monitoring in recent years

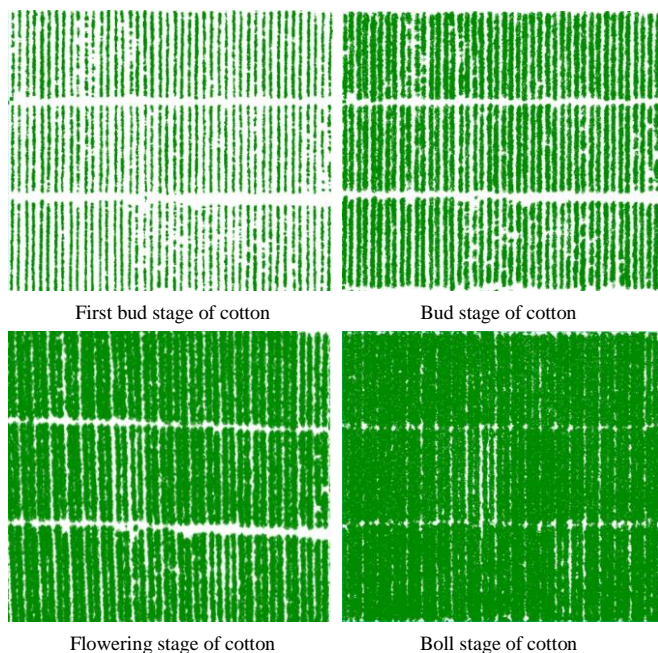


Figure 13 Extraction results of cotton FVC based on TRVI in four periods

due to its advantages of flexibility and low price. For example, Zhang et al.<sup>[13]</sup> constructed the NGRVI index to analyze the differences between the soil and vegetation in the Ebinur Lake basin photo taken by the DJI Phantom4pro visible light system (FVC extraction accuracy was 93.50%, Kappa coefficient was 0.82). Feng et al.<sup>[36]</sup> successfully extracted the FVC of the urban visible light image obtained by the River-Map UAV system through a combination of Random Forest and texture features.

The construction principle of common visible light band vegetation index is based on the strong reflection of vegetation in the green band and the absorption in the yellow and blue bands, and common visible light can enhance vegetation information and minimize non-vegetation information through certain mathematical transformations. The common visible band vegetation index does not consider the effect of shadows on the extraction accuracy of FVC. Therefore, to improve the accuracy of the cotton vegetation information extraction in the first bud stage, bud stage, flowering stage and boll stage of cotton, we should consider how to eliminate the influence of shadow on the extraction of cotton FVC, and select appropriate threshold to extract FVC of cotton.

In this study, the developed TRVI vegetation index comprehensively took into account the spectral differences of soil, shadow and cotton in the research field. The proposed vegetation index threshold method could quickly extract the FVC information of the above-mentioned four periods. The constructed TRVI vegetation index combined with the vegetation index threshold method, which could quickly and effectively extract the FVC of the four periods of cotton.

The constructed TBVI, which combined with the vegetation index threshold method, had pretty low accuracy in extracting cotton FVC. The main reason for the low accuracy was that the difference between the soil and vegetation gray values in the areas of low FVC was not obvious. The Random Forest classification result and TBVI grayscale images of some test areas are shown in Figure 14. The green part in the Random Forest classification image represents cotton, and the white part represents soil.

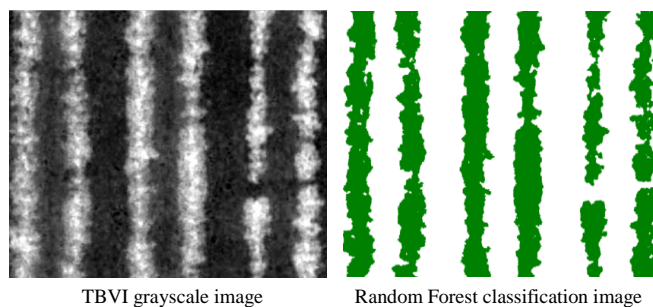


Figure 14 Comparison results of TBVI gray image and Random Forest classification image

## 5 Conclusions

TRVI was successfully constructed in this study based on the spectral differences of soil, shadow and vegetation in the visible light images of the cotton bud stage. The TRVI combined with the vegetation index threshold method was used to extract FVC of cotton first bud stage, bud stage, flowering stage and boll stage. TRVI had a better extraction effect of FVC in the four cotton periods (FVC extraction precision in the first bud stage of cotton with  $R^2$  of 0.832,  $RMSE$  of 0.832, and  $nRMSE$  of 4.405%. The extraction precision  $R^2$  of FVC was 0.981,  $RMSE$  was 1.393 and  $nRMSE$  was 1.984%. FVC extraction precision in the flowering stage of cotton with  $R^2$  of 0.893,  $RMSE$  of 2.101, and  $nRMSE$  of 2.422%. FVC extraction precision in the boll stage of cotton with  $R^2$  of 0.958,  $RMSE$  of 1.850, and  $nRMSE$  of 2.050%. The results show that TRVI combined with vegetation index threshold method not only has high accuracy, but also is easy to operate, and can effectively complete FVC monitoring.

## Acknowledgements

The authors gratefully acknowledge the financial support provided by Top Talents Program for One Case One Discussion of Shandong Province, China Agriculture Research System (Grant No. CARS-15-22), Natural Science Foundation of Shandong Province (Grant No. ZR2021MD091).

## [References]

- [1] Zhang L Z, Spiertz J H J, Zhang S P, Li B, Van der Werf W. Nitrogen economy in relay intercropping systems of wheat and cotton. *Plant and Soil*, 2008; 303(1): 55–68.
- [2] Yoshino M. Agroclimatology problems in the Taklimakan Desert and its surrounding area in NW China. *Journal of Agricultural Meteorology*, 2005; 61(1): 1–14.
- [3] Purevdorj T S, Tateishi R, Ishiyama T, Honda Y. Relationships between percent vegetation cover and vegetation indices. *International Journal of Remote Sensing*, 1998; 19(18): 3519–3535.
- [4] Zhang X, Liao C, Li J, Sun Q. Fractional vegetation cover estimation in arid and semi-arid environments using HJ-1 satellite hyperspectral data. *International Journal of Applied Earth Observation and Geoinformation*, 2013; 21: 506–512.
- [5] Wang X, Jia K, Liang S, Zhang Y. Fractional vegetation cover estimation method through dynamic Bayesian network combining radiative transfer model and crop growth model. *IEEE Transactions on Geoscience and Remote Sensing*, 2016; 54(12): 7442–7450.
- [6] Wang X, Jia K, Liang S, Li Q, Wei X, Yao Y, Tu Y. Estimating fractional vegetation cover from landsat-7 ETM+ reflectance data based on a coupled radiative transfer and crop growth model. *IEEE Transactions on Geoscience and Remote Sensing*, 2017; 55(10): 5539–5546.
- [7] Zhang D, Mansaray L R, Jin H, Sun H, Kuang Z, Huang J. A universal estimation model of fractional vegetation cover for different crops based on time series digital photographs. *Computers and Electronics in Agriculture*, 2018; 151: 93–103.
- [8] Li Y, Xu J, Xia R, Wang X, Xie W. A two-stage framework of target

- detection in high-resolution hyperspectral images. *Signal, Image and Video Processing*, 2019; 13(7): 1339–1346.
- [9] Zhang F, Kung H-T, Johnson V C. Assessment of land-cover/land-use change and landscape patterns in the two national nature reserves of Ebinur Lake Watershed, Xinjiang, China. *Sustainability*, 2017; 9(5): 724. doi: 10.3390/su9050724.
- [10] Zhao J, Yang H B, Lan Y B, Lu L Q, Jia P, Li Z M. Extraction method of summer corn vegetation coverage based on visible light image of unmanned aerial vehicle. *Journal of Agricultural Machinery*, 2019; 50(5): 232–240.
- [11] Yang D J, Zhao J, Lan Y B, Wen Y T, Pan F J, Cao D L, et al. Research on farmland crop classification based on UAV multispectral remote sensing images. *Int J Precis Agric Aviat*, 2021; 4(1): 29–35.
- [12] Santoso F, Redmond S J. Indoor location-aware medical systems for smart homecare and telehealth monitoring: state-of-the-art. *Physiological measurement*, 2015; 36(10): R53–R87.
- [13] Zhang X, Zhang F, Qi Y, Deng L, Wang X, Yang S. New research methods for vegetation information extraction based on visible light remote sensing images from an unmanned aerial vehicle (UAV). *International Journal of Applied Earth Observation and Geoinformation*, 2019; 78: 215–226.
- [14] Yang H B, Zhao J, Lan Y B, Lu L Q, Li Z M. Fraction vegetation cover extraction of winter wheat based on RGB image obtained by UAV. *International Journal of Precision Agricultural Aviation*, 2019; 2(2): 54–61.
- [15] Dorji P, Fearn P. Impact of the spatial resolution of satellite remote sensing sensors in the quantification of total suspended sediment concentration: A case study in turbid waters of Northern Western Australia. *Plos One*, 2017; 12(4): e0175042. doi: 10.1371/journal.pone.0175042.
- [16] Hu J, Yang J. Application of distributed auction to multi-UAV task assignment in agriculture. *International Journal of Precision Agricultural Aviation*, 2018; 1(1): 44–50.
- [17] Choi S K, Lee S K, Jung S H, Choi J W, Choi D Y, Chun S J. Estimation of fractional vegetation cover in sand dunes using multi-spectral images from fixed-wing UAV. *Journal of the Korean Society of Surveying Geodesy Photogrammetry & Cartography*, 2016; 34(4): 431–441.
- [18] Yang H B, Hu X, Zhao J, Hu Y H. Feature extraction of cotton plant height based on DSM difference method. *International Journal of Precision Agricultural Aviation*, 2021; 4(1): 59–69.
- [19] Li B, Liu R, Liu S, Liu Q, Liu F, Zhou G. Monitoring vegetation coverage variation of winter wheat by low-altitude UAV remote sensing system. *Transactions of the CSAE*, 2012; 28(13): 160–165. (in Chinese)
- [20] Du X Y, Wan L, Cen H Y, Chen S B, Zhu J P, Wang H Y, et al. Multi-temporal monitoring of leaf area index of rice under different nitrogen treatments using UAV images. *International Journal of Precision Agricultural Aviation*, 2018; 1(1): 11–18
- [21] Xu W, Lan Y, Li Y, Luo Y, He Z. Classification method of cultivated land based on UAV visible light remote sensing. *International Journal of Agricultural and Biological Engineering*, 2019; 12(3): 103–109.
- [22] Xiang H, Tian L. Development of a low-cost agricultural remote sensing system based on an autonomous unmanned aerial vehicle (UAV). *Biosystems Engineering*, 2011; 108(2): 174–190.
- [23] Tian Z, Fu Y, Liu S. Rapid crops classification based on UAV low-altitude remote sensing. *Transactions of the CSAE*, 2013; 29(7): 109–116. (in Chinese)
- [24] Jones K J. High-scale discontinuity detection applied to Landsat images. In *Wavelet Applications VI*. International Society for Optics and Photonics, 1999; 3723: 114–121.
- [25] Louhaichi M, Borman M M, Johnson D E. Spatially located platform and aerial photography for documentation of grazing impacts on wheat. *Geocarto International*, 2001; 16(1): 65–70.
- [26] Meyer G E, Neto J C. Verification of color vegetation indices for automated crop imaging applications. *Computers and Electronics in Agriculture*, 2008; 63(2): 282–293.
- [27] Tucker C J. Red and photographic infrared linear combinations for monitoring vegetation. *Remote Sensing of Environment*, 1979; 8(2): 127–150.
- [28] Michael, Schirrmann, Antje, et al. Monitoring agronomic parameters of winter wheat crops with low-cost UAV imagery. *Remote Sensing*, 2016, 8(9): 706. doi: 10.3390/rs8090706.
- [29] Tian Z, Fu Y, Liu S. Rapid crops classification based on UAV low-altitude remote sensing. *Transactions of the CSAE*, 2013; 29(7): 109–116. (in Chinese)
- [30] Rundquist B C. The influence of canopy green vegetation fraction on spectral measurements over native tallgrass prairie. *Remote Sensing of Environment*, 2002; 81(1): 129–135.
- [31] Song W, Mu X, Ruan G, Gao Z, Li L, Yan G. Estimating fractional vegetation cover and the vegetation index of bare soil and highly dense vegetation with a physically based method. *International Journal of Applied Earth Observation and Geoinformation*, 2017; 58: 168–176.
- [32] Jia K, Li Y, Liang S, Wei X, Mu X, Yao Y. Fractional vegetation cover estimation based on soil and vegetation lines in a corn-dominated area. *Geocarto International*, 2017; 32(5): 531–540.
- [33] Zhou Q, Robson M. Automated rangeland vegetation cover and density estimation using ground digital images and a spectral-contextual classifier. *International Journal of Remote Sensing*, 2001; 22(17): 3457–3470.
- [34] Zhao F A, Zhang X M, Mu X D, Yao X Y, Zhou Y. Learning multi-modality features for scene classification of high-resolution remote sensing images. *Journal of Computer and Communications*, 2018; 6(11): 185–193.
- [35] Niu Y X, Zhang L Y, Han W T. A novel method for extracting green fractional vegetation cover from digital images. *Journal of Vegetation Science*, 2018; 23 (3): 406–418.
- [36] Feng Q L, Liu J T, Gong J H. UAV remote sensing for urban vegetation mapping using random forest and texture analysis. *Remote Sensing*, 2015; 7(1): 1074–1094.